Probing Molecular Frame Photoionization via Laser Generated High-Order Harmonics from Aligned Molecules

Anh-Thu Le,[1] R. R. Lucchese,[2] M. T. Lee,[3] and C. D. Lin[1]

[1]*Department of Physics, Cardwell Hall, Kansas State University, Manhattan, Kansas 66506, USA*
[2]*Department of Chemistry, Texas A&M University, College Station, Texas 77843-3255, USA*
[3]*Departamento de Química, Universidade Federal de São Carlos, 13565-905, São Paulo, Brazil*

(Received 9 January 2009; published 20 May 2009)

Present experiments cannot measure molecular frame photoelectron angular distributions (MFPAD) for ionization from the outermost valence orbitals of molecules. We show that the details of MFPAD can be retrieved with high-order harmonics generated by infrared lasers from aligned molecules. Using accurately calculated photoionization transition dipole moments for fixed-in-space molecules, we show that the dependence of the magnitude and phase of the high-order harmonics on the alignment angle of the molecules observed in recent experiments can be quantitatively reproduced. This result provides the needed theoretical basis for ultrafast dynamic chemical imaging using infrared laser pulses.

DOI: 10.1103/PhysRevLett.102.203001 PACS numbers: 33.80.Eh, 42.65.Ky

Photoionization (PI) is the basic process that allows direct investigation of molecular structure. Measurements of total, partial, and differential PI cross sections have a long history. Until recently, however, almost all experiments have been performed from an ensemble of randomly oriented molecules. Thus the rich dynamical structure of photoelectron angular distributions for fixed-in-space molecules predicted in the seminal paper by Dill [1] more than 30 years ago still remains largely unexplored. In recent years, fixed-in-space PI has been investigated with x-ray or VUV photons by using the photoelectron-photoion coincidence technique [2–4]. Following inner-shell or inner-valence-shell ionization the molecular ion dissociates. The molecular axis at the time of ionization is inferred from the direction of motion of the fragment ion if the dissociation time is short compared to the rotational period. Clearly this method is not applicable to PI from the highest occupied molecular orbital (HOMO).

Consider the photoionization of a linear molecule. For polarized light, the differential cross section can be expressed in the general form [5] (atomic units are used throughout, unless otherwise indicated)

$$\frac{d^2\sigma}{d\Omega_{\boldsymbol{k}} d\Omega_{\boldsymbol{n}}} = \frac{2(2\pi)^3 E}{3c} \left| \sum_{lm\mu} I_{lm\mu} Y^*_{lm}(\Omega_{\boldsymbol{k}}) Y^*_{1\mu}(\Omega_{\boldsymbol{n}}) \right|^2. \quad (1)$$

In this expression, the molecular axis is fixed and the directions of light polarization and electron emission are given by $\Omega_{\boldsymbol{n}}$ and $\Omega_{\boldsymbol{k}}$, respectively. This is called the molecular frame photoionization angular distribution (MFPAD). We calculate the continuum wave function $\Psi^-_{f,klm}$ and the dipole matrix elements $I_{lm\mu} = k^{1/2}\langle \Psi_i | r_\mu | \Psi^-_{f,klm} \rangle$ using the iterative Schwinger variational method [5] within the complete-active-space configuration interaction scheme [6]. To compare with measurements, integration of Eq. (1) over unobserved variables must be performed, thus losing much valuable information on the structure of the molecule.

In this Letter we show that recent advances in the generation of high-order harmonics from molecules by intense infrared lasers have made it possible to probe fixed-in-space molecular PI from a HOMO. Gas phase molecules can be impulsively aligned by a short subpicosecond infrared laser [7]. After the pulse is turned off, molecules will be partially aligned or antialigned at the time intervals of rotational revivals [8,9]. During these revivals which last for tens or hundreds of femtoseconds, another probe pulse can be used to illuminate molecules to observe the emission of high-order harmonics. The first experiment of this type was reported by Kanai *et al.* [9] using N_2, O_2, and CO_2 molecules. Since then many more experiments have been reported [8,10–14]. To study the dependence of high-order harmonics generation (HHG) on the alignment of molecules, the probe laser can be applied at different times as the molecules evolve, or by changing the direction of the probe laser polarization at a fixed time delay. More recently, HHG from mixed gases [11,12] and interferometry techniques [13] have also been used such that the phase of the HHG can also be measured.

HHG is a highly nonlinear process and can be understood using the three-step model [15]. Electrons are first released from the molecule by tunnel ionization and thrown into the laser field. As the laser's electric field changes direction, the electrons may be driven back to the ion core after gaining kinetic energy from the field. When the electrons recombine with the ion, high-order harmonic photons are emitted. Since the photorecombination (PR) in the last step is the time-reversed process of PI, it is expected that HHG spectra hold valuable information about the molecule. Indeed, HHG spectra have been used to extract the HOMO in N_2 using a tomographic method [16]. However, the tomographic method depends on ap-

 © 2009 The American Physical Society

proximating the continuum electrons by plane waves which are known to fail in general for PI studies. In [17,18] we have developed a quantitative rescattering theory (QRS) for HHG where the complex HHG dipole moment $D(\omega, \theta)$ from a fixed-in-space molecule can be expressed as a product of the transition dipole $d(\omega, \theta) = \sum_{lm\mu} I_{lm\mu} Y^*_{lm}(\Omega_{\boldsymbol{k}}) Y^*_{1\mu}(\Omega_{\boldsymbol{n}})$ (with $\boldsymbol{k} \parallel \boldsymbol{n}$) and the returning electron wave packet $W(E_k, \theta)$,

$$D(\omega, \theta) = W(E_k, \theta) d(\omega, \theta). \quad (2)$$

This model establishes the relation between the induced dipole moment and the transition dipole for PR (or PI). Here θ is the alignment angle of the molecular axis with respect to the polarization direction of the probe laser, $\omega = I_p + E_k$, and where ω is the photon energy of the harmonics, I_p is the ionization potential, and $E_k = k^2/2$ is the "incident" energy of the returning electron. The validity of this equation has been established for atomic targets (no θ dependence for atoms) [17,18] as well as for the H_2^+ target [19]. In both cases, HHG spectra can be calculated accurately by solving the time-dependent Schrödinger equation (TDSE). In this Letter, we obtain the transition dipole $d(\omega, \theta)$ from state-of-the-art PI calculations. The wave packet $W(E_k, \theta)$ is obtained from the strong-field approximation (SFA) [17,19,20]. We then use Eq. (2) to obtain $D(\omega, \theta)$ for each fixed-in-space molecule. To compare with experiments, a proper coherent convolution with the partial alignment of the molecules must be carried out [see Eq. (2) of Ref. [11]].

In Fig. 1(a), we show the theoretical CO_2 PI differential cross section with the emission direction parallel to the light polarization direction ($\boldsymbol{k} \parallel \boldsymbol{n}$), which are compared to HHG data below. By changing the orientation of the fixed-in-space molecule, complementary information on the angular distribution of photoelectrons from fixed-in-space molecules is obtained. In order to compare with HHG data, the photon energies are expressed in units of the photon energy of an 800-nm laser (1.55 eV). First, we note that the differential cross section is large when the alignment angle of the molecule is large. The cross sections vanish at $\theta = 0$ and $\pi/2$ due to the π_g symmetry of the HOMO and the dipole selection rule for the final state. Second, the cross section shows near-zero minima for angles around 35° to 45° for harmonics above the 25th order, or H25. The position of the minimum moves to a larger angle, as the energy increases. These minima have been interpreted as evidence of interference of electron waves from the atomic centers. However, the two-center interference model is not guaranteed to work *a priori*, for example, in N_2. In Fig. 1(b), we show the phase of the PI transition dipole vs photon energy, for alignment angles from 20° to 60°. Between 30° and 45° the dipole phase undergoes rapid change between H25 and H39. This is the region where the cross sections are near the minima [see Fig. 1(a)]. The phase change is about 2.0 to 2.5, instead of π as expected if the cross section indeed goes to zero. For

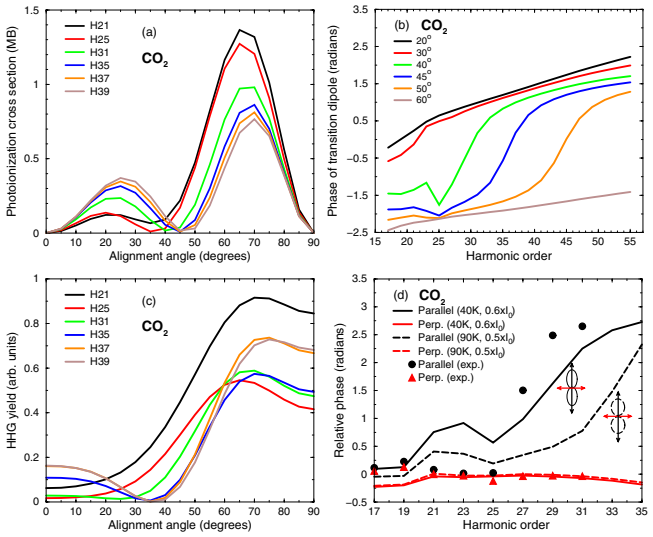

FIG. 1 (color online). CO_2 differential photoionization cross section (a) and phase of the transition dipole (b). The photon energies are expressed in units of harmonic orders for an 800-nm laser. (c) HHG yield as a function of the angle between pump and probe laser polarization directions. The laser intensity and duration are $0.55I_0$ ($I_0 = 10^{14}$ W/cm^2), and 120 fs for the pump pulse, and $2.5I_0$ and 25 fs for the probe pulse. Rotational temperature is taken to be 105 K. (d) Harmonic phase (relative to the phase from Kr) for parallel aligned and perpendicular aligned ensembles, under two sets of parameters (solid and dashed lines) that lead to two alignment distributions. Experimental data from Boutu *el al.* [14] are shown as symbols. Calculations are carried out with the same probe laser parameters as in the experiments.

angles below 20° and above 60° the phase evolves smoothly vs photon energy. The "rich" structures in the theoretical amplitude and phase of $d(\omega, \theta)$ shown in Fig. 1 have never been observed directly in PI experiments. Below we show that they have been observed in recent HHG measurements.

In Fig. 1(c) we show the simulated typical HHG yields from aligned CO_2, as a function of the angle between the pump and probe laser polarization directions. These results are consistent with recent experiments [14,21,22]. Earlier theoretical calculations [23–25] also indicate HHG peaks for large angles. The results also resemble the data for the induced dipole retrieved from mixed-gases experiments by Wagner *et al.* [11] (see their Fig. 4). In our simulation, the laser parameters are taken from the experiment of [13]. The alignment distribution is obtained from numerical solution of the TDSE within the rotor model [7,23,24]. At the delay time corresponding to the maximum alignment near half-revival (1/2 of the rotational period), a probe beam with polarization direction varying from 0° to 90° is used to generate high-order harmonics. Comparing Fig. 1(c) with Fig. 1(a), we note that the HHG yields follow the general angular and photon energy dependence of the differential PI cross sections. Both figures show large yields at large angles, and minima

near 35° for harmonic orders above H31. Because of the averaging over the molecular alignment distributions, the angular dependence of HHG is smoother.

We next show that the phase of a fixed-in-space PI transition dipole can also be probed by comparing to the phase of the harmonics. Experimentally the phases of the harmonics can be extracted from measurements of HHG using mixed gases [12,14] or an interferometry method [13]. In Fig. 1(d), we show the recent experimental data of Boutu *et al.* [14] where the phases of the harmonics (relative to that from Kr) are obtained for ensembles aligned parallel and perpendicular to the field, shown by black and red (or gray) symbols, respectively. For the latter, the phase does not change much in the range of H17 to H31. For the parallel aligned molecules, the phase jump from H17 to H31 was reported to be 2.0 ± 0.6 radians (in the figure it was shown at 2.6 radians). Our simulation results are shown for two different ensembles, with alignment distributions confined in a cone angle of 25° and 35° at half maximum, resulting from different pump beams and gas temperatures (see labels). From Fig. 1(d), we note that for a fixed harmonic, the phase from the parallel aligned ensemble is larger if the angular spread of the molecular distributions is smaller. Therefore, the position of the phase jump for the less aligned ensemble (dashed line) is slightly shifted to higher energies. For the perpendicularly aligned molecules, the phase is small and does not change much with the harmonic order. This is consistent with the phase shown in Fig. 1(b). Thus the phase of HHG in Fig. 1(d) is seen to mimic the phase of the PI transition dipole shown in Fig. 1(b).

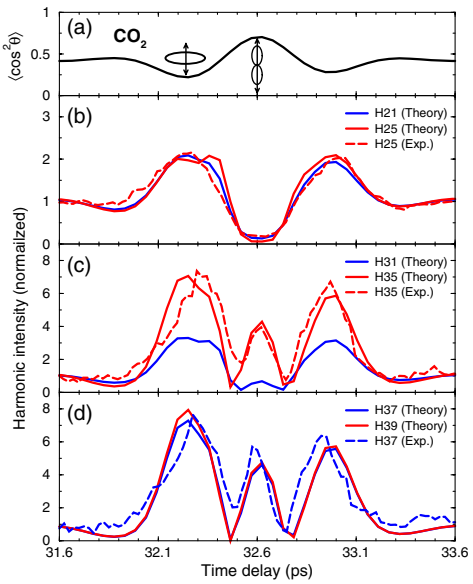

FIG. 2 (color online). Normalized HHG yield (vs isotropically distributed molecules) from CO_2 for different harmonics as a function of pump-probe delay time near the 3/4 revival. Laser parameters are the same as in Fig. 1(c). The experimental data are taken from Zhou *et al* [13]. The alignment parameter $\langle\cos^2\theta\rangle$ is plotted for reference (a).

Next we show in Fig. 2 how the HHG yields change with the time delay near the 3/4 revival where the molecule can be most strongly aligned. Our simulations were carried out with the laser parameters from Zhou *et al.* [13]. The degree of alignment (top panel), as measured by $\langle\cos^2\theta\rangle$ has a maximum when the molecules are maximally aligned (vertically in the figure) and has a minimum when the molecules are antialigned. Our results are shown for the same harmonics that were analyzed in [13] (see their Fig. 2—according to a new assignment by the authors of [13], the harmonic orders should be properly shifted down by two orders, compared to the ones given in their original paper [22]). For the lower harmonics H21 and H25, the yields follow the inverse of the alignment parameter. This is easily understood from Fig. 1(a) which shows that the PI cross sections at large angles are much larger than at small angles. For the higher orders, Fig. 1(a) indicates that the PI cross sections show two humps, with the one at smaller angles only a factor of about 2 to 3 times smaller than the other. Qualitatively, this explains why the HHG yields for H31 and higher show a pronounced peak for the parallel alignment. We note a quantitatively good agreement between our calculations and the experimental data.

The evolution of the HHG yields was also studied by Wagner *et al.* [11] using the mixed-gases technique. The yield and phase for H31 vs time delay near the half-revival are shown in Figs. 3(c) and 3(b), respectively. Our simulations (solid lines) are also in good agreement with these measurements. The HHG yield is small when the molecules are maximally aligned. This is in agreement with H31 seen in Fig. 2(c) for the delay time near the 3/4 revival. However, we note that the phase has a maximum when the molecules are maximally aligned. This can be understood from the phase in Fig. 1(b) where it is shown that the phase is large when the alignment angle is small. It also shows that the phase is small when the alignment angle is large; thus, for antialigned molecules the phase

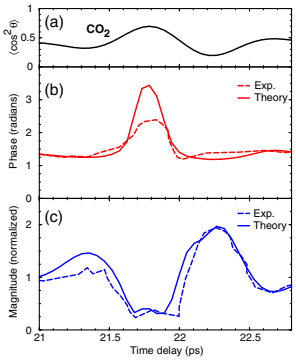

FIG. 3 (color online). Alignment parameter $\langle\cos^2\theta\rangle$ (a), phase (b), and magnitude (c) of the 31th order harmonic from CO_2, as functions of pump-probe delay time near the half-revival. The experimental data are taken from Wagner *et al* [11]. The laser intensity and duration are $0.38 \times I_0$ and 140 fs for the pump, and $2.5 \times I_0$ and 30 fs for the probe. The rotational temperature is taken to be 70 K.

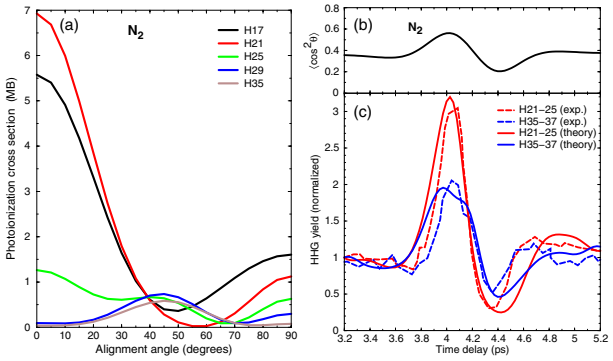

FIG. 4 (color online). (a) Same as in Fig. 1(a), but for N_2. (b), (c): Alignment parameter $\langle \cos^2\theta \rangle$ and harmonic yields H21–H25 and H35–H37 from N_2. The experimental data and laser parameters are taken from Itatani *et al* [8].

of the HHG should be small, as seen in the experimental data and in the simulation.

We remark that the laser intensity used in the JILA experiment [13] is quite high; thus, the effect of the depletion of the ground state by the laser should be considered [23,24,26]. For CO_2, the alignment dependence of the ionization rate is still not fully settled. The results from the molecular tunneling ionization (MO-ADK) theory [27], the SFA theory and the experiment [28] all disagree with each other, with the SFA predicting a peak near 40°, compared to 30° from the MO-ADK theory, and 45° from experiment [28]. Using ionization rates from MO-ADK, we have not been able to simulate the experimental data accurately. We thus used ionization rates from SFA, except that we renormalize the SFA rate to that of the MO-ADK rate at laser intensity of I_0, which gives a factor of 10. Note that the same correction factor has been found for the SFA ionization from Kr, which has almost the same ionization potential as CO_2. With the corrected SFA rate, we found that our simulations give a better quantitative agreement with the JILA data [13].

We have also studied N_2 molecules. The fixed-in-space differential PI cross sections are shown in Fig. 4(a). For H17 to H21, the cross sections are quite large since this is in the tail region of the famous shape resonance in N_2. For these orders, the cross sections are highly forward peaked. For energies above H25, the cross sections become much smaller, and they are of the same order of magnitude for the parallel and perpendicular alignments. However, note that the cross sections have minima at large angles around 60°—70°. The (normalized) HHG spectra of N_2 has been measured vs time delay in [8]. Their results are shown in Fig. 4(c), along with the results from our simulation. Clearly for H21-H25, the yield (normalized to the isotropic distribution case) is much larger than that from the higher harmonics when the molecules are maximally aligned, which is consistent with the PI cross sections shown in Fig. 4(a). Once again, the experimental HHG spectra can be reproduced within the QRS based on the accurate dipole transition amplitudes from PI calculation, thus allowing us to probe the MFPAD for ionization from the HOMO.

In conclusion, we have shown that molecular frame photoionization can be probed directly using laser-generated high-order harmonics from aligned molecules. This method is particularly useful for probing fixed-in-space molecular photoionization from the HOMOs. Alternatively, using accurate PI dipole matrix elements calculated from the state-of-the-art molecular photoionization codes, we have illustrated that the nonlinear HHG spectra can be accurately calculated [see Eq. (2)]. By varying laser intensity, HHG spectra from lower-lying orbitals can also be similarly probed [29]. Having established the connection between HHG and the PI dipole matrix elements, see Eq. (2), time-resolved PI cross sections can be extracted from HHG spectra in a typical pump-probe experimental setup, thus opening up the opportunity of using infrared laser pulses for ultrafast dynamic chemical imaging.

We thank X. Zhou, N. Wagner, M. Murnane, H. Kapteyn, and P. Salieres for communicating their results to us and the valuable discussions. This work was supported in part by the Chemical Sciences, Geosciences and Biosciences Division, Office of Basic Energy Sciences, Office of Science, U.S. Department of Energy.

[1] D. Dill, J. Chem. Phys. **65**, 1130 (1976).
[2] T. Weber *et al.*, Nature (London) **431**, 437 (2004).
[3] D. Rolles *et al.*, Nature (London) **437**, 711 (2005).
[4] X.-J. Liu *et al.*, Phys. Rev. Lett. **101**, 023001 (2008).
[5] R. R. Lucchese *et al.*, Phys. Rev. A **25**, 2572 (1982).
[6] R. E. Stratmann and R. R. Lucchese, J. Chem. Phys. **102**, 8493 (1995).
[7] H. Stapelfeldt and T. Seideman, Rev. Mod. Phys. **75**, 543 (2003).
[8] J. Itatani *et al.*, Phys. Rev. Lett. **94**, 123902 (2005).
[9] T. Kanai *et al.*, Nature (London) **435**, 470 (2005).
[10] C. Vozzi *et al.*, Phys. Rev. Lett. **95**, 153902 (2005).
[11] N. Wagner *et al.*, Phys. Rev. A **76**, 061403 (2007).
[12] T. Kanai *et al.*, Phys. Rev. A **77**, 041402 (2008).
[13] X. Zhou *et al.*, Phys. Rev. Lett. **100**, 073902 (2008).
[14] W. Boutu *et al.*, Nature Phys. **4**, 545 (2008).
[15] P. B. Corkum, Phys. Rev. Lett. **71**, 1994 (1993).
[16] J. Itatani *et al.*, Nature (London) **432**, 867 (2004).
[17] A. T. Le *et al.*, Phys. Rev. A **78**, 023814 (2008).
[18] T. Morishita *et al.*, Phys. Rev. Lett. **100**, 013903 (2008).
[19] A. T. Le *et al.*, J. Phys. B **41**, 081002 (2008).
[20] M. Lewenstein *et al.*, Phys. Rev. A **49**, 2117 (1994).
[21] Y. Mairesse *et al.*, J. Mod. Opt. **55**, 2591 (2008).
[22] X. Zhou and M. Murnane (private communication).
[23] A. T. Le *et al.*, Phys. Rev. A **73**, 041402(R) (2006).
[24] A. T. Le *et al.*, J. Mod. Opt. **54**, 967 (2007).
[25] R. de Nalda *et al.*, Phys. Rev. A **69**, 031804(R) (2004).
[26] P. Liu *et al.*, Phys. Rev. A **78**, 015802 (2008).
[27] X. M. Tong *et al.*, Phys. Rev. A **66**, 033402 (2002).
[28] D. Pavicic *et al.*, Phys. Rev. Lett. **98**, 243001 (2007).
[29] B. K. McFarland *et al.*, Science **322**, 1232 (2008).